Nuclear electric dipole moments for the lowest $1/2^+$ states in Xe and Ba isotopes

N. Yoshinaga,[1,*] K. Higashiyama,[2,†] R. Arai,[1] and E. Teruya[1]
[1]*Department of Physics, Saitama University, Saitama City 338-8570, Japan*
[2]*Department of Physics, Chiba Institute of Technology, Narashino, Chiba 275-0023, Japan*
(Received 9 February 2014; published 9 April 2014)

The electric dipole moments for the lowest $1/2^+$ states of Xe and Ba isotopes are calculated in terms of the nuclear shell model, which includes two-body nucleon interactions violating parity and time-reversal invariance. Using the wave functions thus obtained, the nuclear electric dipole moments arising from the intrinsic nucleon electric dipole moments and also from asymmetric charge distribution are calculated. The upper limits for the nuclear electric dipole moments of Xe and Ba isotopes are estimated.

DOI: 10.1103/PhysRevC.89.045501 PACS number(s): 21.10.Ky, 11.30.Er, 21.60.Cs, 27.60.+j

I. INTRODUCTION

The search for interactions violating time reversal (T) invariance is an important part of studies of fundamental symmetries in nature. The Standard Model in particle physics violates charge conjugation and parity (CP) invariance, but only through a single phase in the Kobayashi-Maskawa matrix that mixes quark flavors [1]. Nevertheless, it is too weak to explain the matter-antimatter asymmetry of the Universe [2,3]. The resulting T violation is therefore expected to be very weak as long as the CPT theorem holds. The manifestations of CP violation (and therefore, through the CPT theorem, of T violation) in systems of neutral K and B mesons [4] set limits on physical effects beyond the Standard Model. The main hopes for the extraction of nucleon-nucleon and quark-quark interactions violating fundamental symmetries emerge from the experiments with atoms and atomic nuclei [5,6]. For example, the best limits on P- and T-odd forces have been obtained from the measurements of the atomic electric dipole moments (EDMs) in the ^{199}Hg [7] and ^{129}Xe [8] nuclei. With a new device, experimental efforts searching for an atomic EDM of ^{129}Xe are now in progress [9].

Recently it was reported that the nuclear EDM would be measured directly by using an ionic atom instead of a neutral atom [10,11]. For a neutral atom the nuclear EDM is completely shielded by the surrounding electrons due to the Schiff theorem [12]. However, for an ionic atom the nuclear EDM is not shielded completely by electrons and thus it is meaningful to measure the EDM of the ionic atom [13]. Fujita and Oshima recently calculated the nuclear EDMs of neutron odd nuclei with even protons in a phenomenological shell model picture, assuming a relation between the nuclear EDMs and the magnetic moments [14].

In the previous paper, the nuclear wave functions for Xe isotopes were calculated in terms of the nuclear shell model, in which two-body interactions violating P and T invariance were included in additional to ordinary nuclear forces [15]. Using wave functions thus obtained, the Schiff moments for the lowest $1/2^+$ states of Xe isotopes were calculated. The Schiff moments were utilized to give upper limits of atomic EDMs for Xe isotopes.

*yoshinaga@phy.saitama-u.ac.jp
†koji.higashiyama@it-chiba.ac.jp

The nuclear EDM is induced by two different sources of mechanism. One originates from the intrinsic nucleon EDM, which was partly reported in Ref. [16]. The other comes from the two-body nuclear interaction which violates P and T invariance. In the present paper the EDMs for the lowest $1/2^+$ states of Xe and Ba isotopes are calculated in terms of the nuclear shell model from two different sources.

The paper is organized as follows. In Sec. II, the framework of the nuclear shell model is reviewed. In Sec. III the method of calculating EDMs is described. In Sec. IV numerical results are given for the EDMs. Principal results are discussed and summarized in Sec. V.

II. SHELL MODEL FRAMEWORK

The nuclear shell model is one of the most appropriate approaches for describing various aspects of nuclear structure. However, the full-fledged shell model calculation in the mass $A \sim 130$ region is impractical at present because of its huge dimension of configuration space. To describe the $A \sim 130$ nuclei, we adopt the pair truncated shell model [17–19]. In this model the full shell model space is restricted to the subspace of collective pairs. A nucleon pair creation operator with total angular momentum J and its projection M is defined as

$$\hat{A}^{\dagger(J)}_M(j_1 j_2) = \sum_{m_1 m_2} (j_1 m_1 j_2 m_2 | J M) \hat{c}^\dagger_{j_1 m_1} \hat{c}^\dagger_{j_2 m_2}, \qquad (1)$$

where $\hat{c}^\dagger_{jm}$ stands for the nucleon creation operator in the j orbital with its projection m and $(j_1 m_1 j_2 m_2 | J M)$ stands for a Clebsch-Gordan coefficient. Using this pair, the collective nucleon pair creation operators with angular momenta zero (S) and two (D) are defined as

$$\hat{S}^\dagger = \sum_j \alpha_j \hat{A}^{\dagger(0)}_0(jj), \qquad (2)$$

$$\hat{D}^\dagger_M = \sum_{j_1 j_2} \beta_{j_1 j_2} \hat{A}^{\dagger(2)}_M(j_1 j_2), \qquad (3)$$

where the structure coefficients α and β are determined by variation in the present approach.

The model space includes the five levels $0g_{7/2}$, $1d_{5/2}$, $1d_{3/2}$, $0h_{11/2}$, and $2s_{1/2}$ in the major shell between the magic numbers 50 and 82. In addition, four levels for protons, $1f_{7/2}$, $1f_{5/2}$,

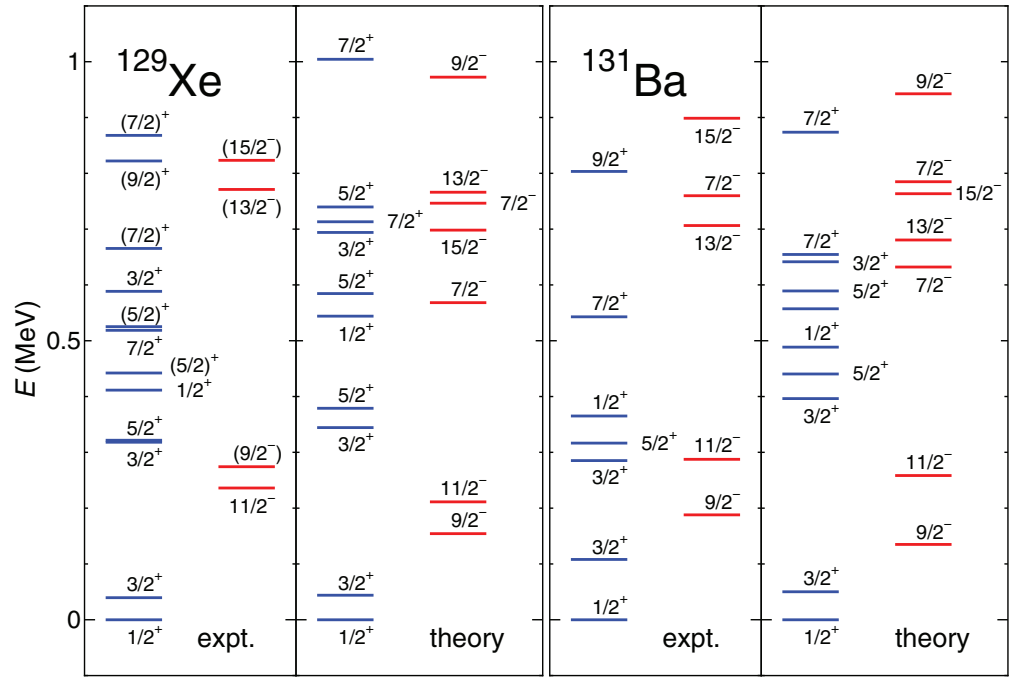

FIG. 1. (Color online) Comparison of the experimental energy levels (expt.) with those of the shell model (theory) for ^{129}Xe and ^{131}Ba. The experimental data are taken from Refs. [20–22].

$2p_{3/2}$, and $2p_{1/2}$, are taken into account above the closed shell $Z = 82$. For a description of negative-parity states, we introduce proton negative-parity (N_k,k = 1,2,3,4,5) pairs

$$\hat{N}^{\dagger(K_1)}_{1M} = \hat{A}^{\dagger(K_1)}_M(g_{7/2}, f_{7/2}), \tag{4}$$

$$\hat{N}^{\dagger(K_2)}_{2M} = \hat{A}^{\dagger(K_2)}_M(d_{5/2}, f_{5/2}), \tag{5}$$

$$\hat{N}^{\dagger(K_3)}_{3M} = \hat{A}^{\dagger(K_3)}_M(s_{1/2}, p_{1/2}), \tag{6}$$

$$\hat{N}^{\dagger(K_4)}_{4M} = \hat{A}^{\dagger(K_4)}_M(g_{7/2}, f_{5/2}), \tag{7}$$

$$\hat{N}^{\dagger(K_5)}_{5M} = \hat{A}^{\dagger(K_5)}_M(d_{5/2}, f_{7/2}), \tag{8}$$

where the coupled angular momenta take values of $K_{1,2}$ = 0,1,2,3,4, K_3 = 0,1 and $K_{4,5}$ = 1,2,3,4. Then the SD+N_k-pair state is constructed as

$$\left|S^{n_s} D^{n_d} N_k^{n_k} I\eta\right\rangle = (\hat{S}^\dagger)^{n_s}(\hat{D}^\dagger)^{n_d}(\hat{N}^\dagger_k)^{n_k}|-\rangle, \tag{9}$$

where $n_s + n_d + n_k$ gives half the number of valence nucleons, I is a total angular momentum, and η is an additional quantum number required to completely specify the state. The angular momentum coupling is carried out exactly, but we abbreviate its notation.

To describe odd-mass nuclei, we add an unpaired nucleon in the j orbital to the SD-pair states. The state is now written as

$$|j S^{n_s} D^{n_d} I\eta\rangle = [\hat{c}^\dagger_j|S^{n_s} D^{n_d} I'\eta\rangle]^{(I)}, \tag{10}$$

where I' is the total angular momentum of the SD pair state, I is the total angular momentum of the SD pair plus one-particle state, and η is an additional quantum number. Using the SD pair plus one-particle state in neutron space and the SD+N_k-pair state in proton space, we can express the many-body wave function of the odd-even (neutron-odd and proton-even) nucleus with a total spin I and its projection M as

$$|\Phi(IM\eta)\rangle = \left[|j_n S^{\bar{n}_s} D^{\bar{n}_d} I_n\eta_n\rangle \otimes \left|S^{n_s} D^{n_d} N_k^{n_k} I_p\eta_p\right\rangle\right]^{(I)}_M, \tag{11}$$

where $2(\bar{n}_s + \bar{n}_d) + 1$ and $2(n_s + n_d + n_k)$ are numbers of valence neutron holes and proton particles, respectively.

As an effective two-body interaction, we employ the monopole and quadrupole pairing plus quadrupole-quadrupole interaction. The effective shell model Hamiltonian is written as

$$\hat{H}_0 = \hat{H}_n + \hat{H}_p + \hat{H}_{np}, \tag{12}$$

where $\hat{H}_n$, $\hat{H}_p$, and $\hat{H}_{np}$ represent the interaction among neutrons, the interaction among protons, and the interaction between neutrons and protons, respectively. The explicit form of the Hamiltonian and the interaction strengths were reported in Ref. [15].

The Hamiltonian in Eq. (12) is diagonalized in terms of the many-body basis wave functions in Eq. (11) as

$$\hat{H}_0\left|I^\pi_k\right\rangle = E\left(I^\pi_k\right)\left|I^\pi_k\right\rangle, \tag{13}$$

where $|I^\pi_k\rangle$ is the normalized eigenvector for the kth state with spin I and parity π, and $E(I^\pi_k)$ is the eigenenergy for the state $|I^\pi_k\rangle$. In Fig. 1, the theoretical energy levels are compared with the experimental data for ^{129}Xe and ^{131}Ba. For both nuclei there exist one-to-one correspondences between the theoretical and

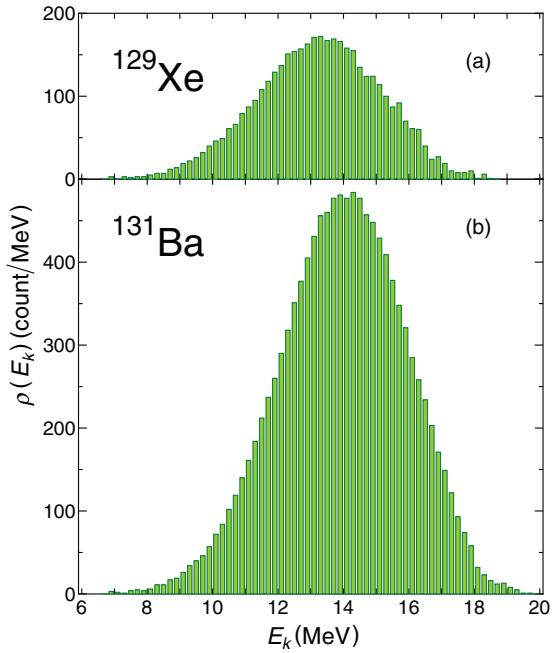

FIG. 2. (Color online) Density of the $1/2^-$ states $\rho(E_k)$ in (a) ^{129}Xe and (b) ^{131}Ba.

experimental levels for the $1/2^+_1$, $3/2^+_1$, $3/2^+_2$, and $5/2^+_1$ states. Concerning the negative-parity states, the level ordering of the $11/2^-_1$ and $9/2^-_1$ states is reversely predicted for ^{129}Xe. In contrast, the shell model calculation reproduces quite well the correct ordering of these states for ^{131}Ba.

The density of the $1/2^-$ states is defined as

$$\rho(E_k) = \left.\frac{dN}{dE}\right|_{E=E_k}, \tag{14}$$

where E_k is the excitation energy $E_k = E(\frac{1}{2}^-_k) - E(\frac{1}{2}^+_1)$. We take $dE = 0.2$ MeV and dN is the number of the $1/2^-$ states in the range dE. In Fig. 2, we show the densities of the $1/2^-$ states for ^{129}Xe and ^{131}Ba. For each nucleus, the density of states, ρ, has a Gaussian shape and increases exponentially between 8 and 12 MeV. At 13 MeV (14 MeV) for ^{129}Xe (^{131}Ba) it becomes maximum, but the contribution of each state above 12 MeV to the EDM is marginal, which is discussed in Sec. IV.

III. ELECTRIC DIPOLE MOMENTS

The nuclear EDM comes from two independent origins. One arises from the asymmetric nuclear charge distribution and the other is induced from the intrinsic nucleon EDM. The EDM operator is expressed as the sum of two terms:

$$\hat{\boldsymbol{D}} = \hat{\boldsymbol{D}}_{\rm ch} + \hat{\boldsymbol{D}}_{\rm int}, \tag{15}$$

where $\hat{\boldsymbol{D}}_{\rm ch}$ originates from the asymmetric nuclear charge distribution

$$\hat{\boldsymbol{D}}_{\rm ch} = \sum_{i=1}^{A} e_i\,(\boldsymbol{r}_i - \boldsymbol{R}). \tag{16}$$

Here A is the mass number of a specific nucleus, and $\boldsymbol{r}_i$ and e_i are the position and the charge for the ith nucleon, respectively. We take $e_i = 0$ for a neutron and $e_i = e$ for a proton. The $\boldsymbol{R}$ represents the center of mass of the nucleus. The $\hat{\boldsymbol{D}}_{\rm int}$ is the EDM operator arising from the intrinsic nucleon EDM, which is expressed as

$$\hat{\boldsymbol{D}}_{\rm int} = \sum_{i=1}^{A} \hat{\boldsymbol{d}}_i. \tag{17}$$

Here $\hat{\boldsymbol{d}}_i$ indicates the intrinsic nucleon EDM operator for the ith nucleon, which is expressed in the nonrelativistic approximation as

$$\hat{\boldsymbol{d}}_i = \tfrac{1}{2}\big[(1-\tau_{iz})d_n\hat{\boldsymbol{\sigma}}^n_i + (1+\tau_{iz})d_p\hat{\boldsymbol{\sigma}}^p_i\big]. \tag{18}$$

Here τ_{iz} represents the third component of isotopic operator, d_n and d_p are the intrinsic EDMs for a neutron and a proton, respectively, and $\hat{\boldsymbol{\sigma}}^t_i$ represents the Pauli spin operator for the neutron ($t = n$) or the proton ($t = p$).

When a nuclear PT-violating two-body interaction is introduced, the total Hamiltonian is now written as

$$\hat{H} = \hat{H}_0 + V^{PT}_{\pi(I)}, \tag{19}$$

where $\hat{H}_0$ is the Hamiltonian in Eq. (12), and $V^{PT}_{\pi(I)}$ is a two-body nuclear interaction violating P and T invariance. We adopt three isospin types [23–25] for the nuclear PT-violating two-body interaction. The isoscalar ($I = 0$), isovector ($I = 1$), and isotensor ($I = 2$) interactions are respectively written as

$$V^{PT}_{\pi(0)} = F_0(\boldsymbol{\tau}_1\cdot\boldsymbol{\tau}_2)(\boldsymbol{\sigma}_1 - \boldsymbol{\sigma}_2)\cdot\boldsymbol{r}\,f(r), \tag{20}$$

$$V^{PT}_{\pi(1)} = F_1[(\tau_{1z}+\tau_{2z})(\boldsymbol{\sigma}_1 - \boldsymbol{\sigma}_2) + (\tau_{1z}-\tau_{2z})(\boldsymbol{\sigma}_1 + \boldsymbol{\sigma}_2)]\cdot\boldsymbol{r}\,f(r), \tag{21}$$

$$V^{PT}_{\pi(2)} = F_2\big(3\tau_{1z}\tau_{2z} - \boldsymbol{\tau}_1\cdot\boldsymbol{\tau}_2\big)(\boldsymbol{\sigma}_1 - \boldsymbol{\sigma}_2)\cdot\boldsymbol{r}\,f(r), \tag{22}$$

where

$$f(r) = \frac{\exp(-m_\pi r)}{m_\pi r^2}\left(1 + \frac{1}{m_\pi r}\right), \tag{23}$$

with $\boldsymbol{r} = \boldsymbol{r}_1 - \boldsymbol{r}_2$, and $r = |\boldsymbol{r}|$. The coefficients F_I are expressed as

$$F_0 = -\frac{1}{8\pi}\frac{m_\pi^2}{M_N}\bar{g}^{(0)}g, \tag{24}$$

$$F_1 = -\frac{1}{16\pi}\frac{m_\pi^2}{M_N}\bar{g}^{(1)}g, \tag{25}$$

$$F_2 = -\frac{1}{8\pi}\frac{m_\pi^2}{M_N}\bar{g}^{(2)}g, \tag{26}$$

where M_N is the mass of a nucleon, m_π is the mass of a pion, g is the strong πNN coupling constant, and $\bar{g}^{(I)}$ with isospin I is the strong πNN constant which breaks P and T invariance.

We treat the nuclear PT-violating two-body interaction as a perturbation. Then the total wave function of the first $1/2^+$

state, $|\frac{1}{2}^+_1\rangle\rangle$, is given as

$$|\tfrac{1}{2}^+_1\rangle\rangle = |\tfrac{1}{2}^+_1\rangle + \sum_{k=1} \frac{1}{E_1^{(+)} - E_k^{(-)}} \langle \tfrac{1}{2}^-_k | V^{PT}_{\pi(I)} | \tfrac{1}{2}^+_1 \rangle | \tfrac{1}{2}^-_k \rangle, \tag{27}$$

where $|\frac{1}{2}^\pi_k\rangle$ is an unperturbed state given by Eq. (13). All these states have projection (spin third component) 1/2. Using the notation in Eq. (13), we identify the energy as $E_k^{(\pi)} = E(\frac{1}{2}^\pi_k)$.

The nuclear EDM for the first $1/2^+$ state is expressed as

$$d_{\rm N} = \langle\langle \tfrac{1}{2}^+_1 | \hat{D}_z | \tfrac{1}{2}^+_1 \rangle\rangle = d_{\rm N,ch} + d_{\rm N,int}. \tag{28}$$

The EDM coming from the intrinsic nucleon EDM, $d_{\rm N,int}$, is expressed as

$$d_{\rm N,int} = \langle\langle \tfrac{1}{2}^+_1 | \hat{D}_{{\rm int},z} | \tfrac{1}{2}^+_1 \rangle\rangle = \langle \tfrac{1}{2}^+_1 | \hat{D}_{{\rm int},z} | \tfrac{1}{2}^+_1 \rangle, \tag{29}$$

where $\hat{D}_{{\rm int},z}$ is the third coordinate component of $\hat{\boldsymbol{D}}_{\rm int}$. The nuclear EDM caused by charge asymmetry, $d_{\rm N,ch}$, is expressed as

$$\begin{aligned} d_{\rm N,ch} &= \langle\langle \tfrac{1}{2}^+_1 | \hat{D}_{{\rm ch},z} | \tfrac{1}{2}^+_1 \rangle\rangle \\ &= \sum_{k=1} \frac{\langle \frac{1}{2}^+_1 | \hat{D}_{{\rm ch},z} | \frac{1}{2}^-_k \rangle \langle \frac{1}{2}^-_k | V^{PT}_{\pi(I)} | \frac{1}{2}^+_1 \rangle}{E_1^{(+)} - E_k^{(-)}} + {\rm c.c.}, \end{aligned} \tag{30}$$

where $\hat{D}_{{\rm ch},z}$ is the third coordinate component of $\hat{\boldsymbol{D}}_{\rm ch}$.

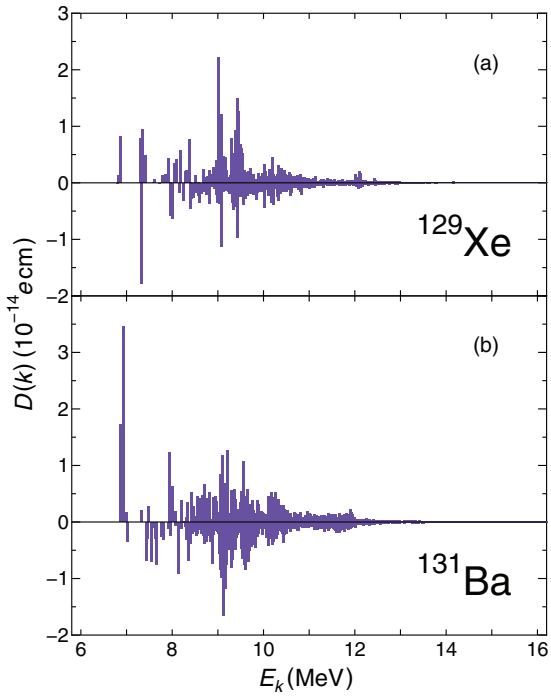

FIG. 3. (Color online) Strength function for the EDM operator in (a) ^{129}Xe and (b) ^{131}Ba.

IV. NUMERICAL RESULTS

We define the partial contribution of the kth state $|\frac{1}{2}^-_k\rangle$ to the EDM by

$$d_{(I)}(k) = \frac{\langle \frac{1}{2}^+_1 | \hat{D}_{{\rm ch},z} | \frac{1}{2}^-_k \rangle \langle \frac{1}{2}^-_k | V^{PT}_{\pi(I)} | \frac{1}{2}^+_1 \rangle}{E_1^{(+)} - E_k^{(-)}} + {\rm c.c.} \tag{31}$$

In evaluating Eq. (31), the strength function for the EDM operator is given by

$$D\,(k) = \langle \tfrac{1}{2}^+_1 | \hat{D}_{{\rm ch},z} | \tfrac{1}{2}^-_k \rangle, \tag{32}$$

which is shown for ^{129}Xe and ^{131}Ba in Fig. 3. There exist several strong strengths in the range between 6 and 10 MeV.

In Fig. 4 we show the off-diagonal potential matrix elements

$$V_{(I)}\,(k) = \langle \tfrac{1}{2}^-_k | V^{PT}_{\pi(I)} | \tfrac{1}{2}^+_1 \rangle, \tag{33}$$

for the isoscalar ($I = 0$) part. In contrast to the strength function for the EDM, there are now two large contributions just above 6.8 MeV (7.0 MeV) in the enlarged scale for ^{129}Xe (^{131}Ba).

In Fig. 5, the partial contribution $d_{(I)}(k)$ to the EDM for the isoscalar ($I = 0$) two-body interaction in ^{129}Xe and ^{131}Ba is shown as a function of the excitation energy E_k ($E_k = E_k^{(-)} - E_1^{(+)}$). The "SUM" indicates the sum of each EDM contribution defined by

$$d^{\rm SUM}_{(I)}(k) = \sum_{i=1}^{k} d_{(I)}(i), \tag{34}$$

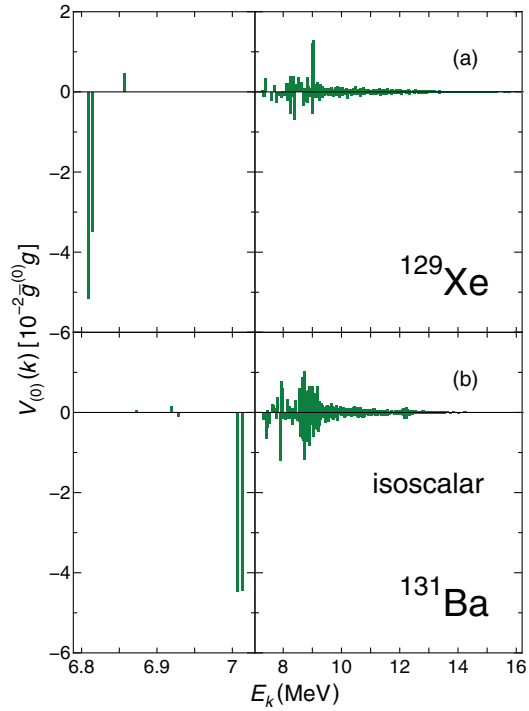

FIG. 4. (Color online) Off-diagonal potential matrix elements between $1/2^+_1$ state and $1/2^-_k$ state for the isoscalar interaction within the energy ranges below 7.03 MeV (left panel) and above 7.03 MeV in (a) ^{129}Xe and (b) ^{131}Ba.

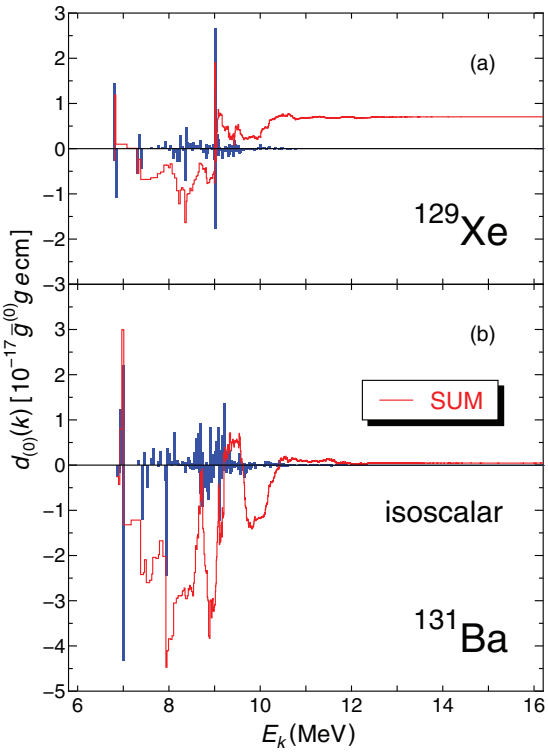

FIG. 5. (Color online) Partial contribution to the EDM for the isoscalar ($I = 0$) type two-body interaction in (a) ^{129}Xe and (b) ^{131}Ba as a function of excitation energies of $1/2^-$ states.

where the summation is taken over contributions from the first state to the kth state with spin $1/2$ and negative parity. Almost no contributions are seen above 12.0 MeV. This behavior is analogous to the Schiff moments studied in the previous paper [15]. The total sum for the isoscalar ($I = 0$) in ^{129}Xe results in

$$d_{\mathrm{N,ch}} = 7.04 \times 10^{-18}\,\bar{g}^{(0)}g\ e\,\mathrm{cm}. \tag{35}$$

In Figs. 6 and 7 we show the partial contributions to the EDMs and their total sums, respectively, for isovector ($I = 1$) and isotensor ($I = 2$) two-body interactions. All three isospin EDMs resemble one another, but especially isovector and isotensor moments look quite similar to each other except for absolute values. In Table I we show the results of EDMs in units of $\bar{g}^{(I)}g\ e\,\mathrm{cm}$ ($I = 0,1,2$) for Xe and Ba isotopes.

As shown in Eq. (28), the contribution to the EDM also comes from the intrinsic nucleon EDM. The nuclear EDM

TABLE I. EDMs in units of $10^{-17}\bar{g}^{(I)}g\ e\,\mathrm{cm}$ ($I = 0,1,2$).

Nucleus	^{129}Xe	^{131}Xe	^{133}Xe	^{135}Xe
Isoscalar ($I = 0$)	0.704	0.027	−0.859	−0.557
Isovector ($I = 1$)	0.735	0.339	−0.161	0.090
Isotensor ($I = 2$)	3.71	2.01	−0.107	1.10
Nucleus	^{131}Ba	^{133}Ba	^{135}Ba	^{137}Ba
Isoscalar ($I = 0$)	0.045	−2.67	−3.58	−4.83
Isovector ($I = 1$)	0.213	−0.826	−1.34	−1.48
Isotensor ($I = 2$)	1.23	−2.29	−4.45	−4.06

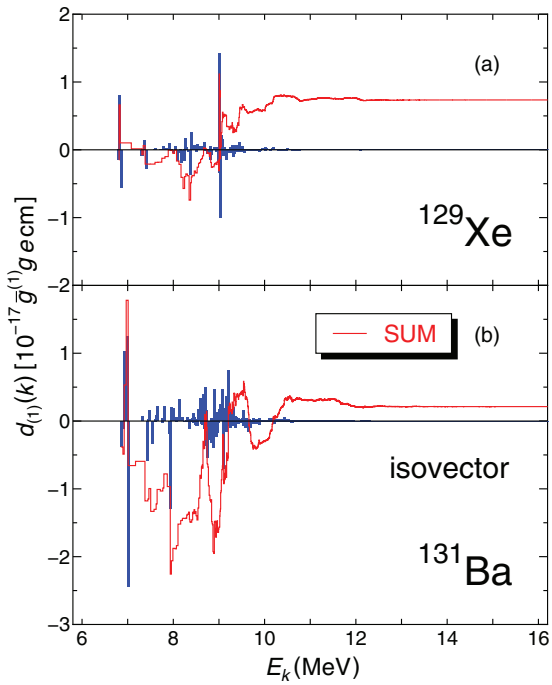

FIG. 6. (Color online) Same as in Fig. 5, but for the isovector ($I = 1$) type two-body interaction.

$d_{\mathrm{N,int}}$ is expressed as

$$d_{\mathrm{N,int}} = \left\langle \tfrac{1}{2}^+_1 \middle| \hat{D}_{\mathrm{int},z} \middle| \tfrac{1}{2}^+_1 \right\rangle = \langle \hat{\sigma}_z^n \rangle d_n + \langle \hat{\sigma}_z^p \rangle d_p, \tag{36}$$

where $\langle \hat{\sigma}_z^t \rangle$ is the expectation value of the spin operator $\hat{\sigma}_z^t$ ($t = n$ or p) in terms of the shell model wave function.

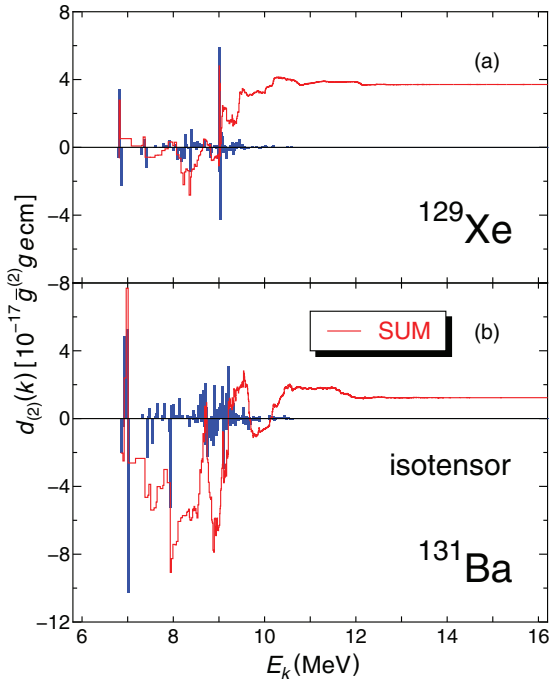

FIG. 7. (Color online) Same as in Fig. 5, but for the isotensor ($I = 2$) type two-body interaction.

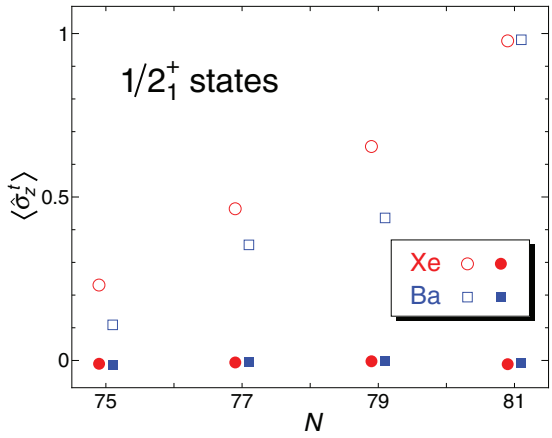

FIG. 8. (Color online) The factors $\langle\hat{\sigma}_z^t\rangle$ ($t = n$ or p) for the Xe and Ba isotopes. The open and filled circles (squares) represent the $\langle\hat{\sigma}_z^n\rangle$ and $\langle\hat{\sigma}_z^p\rangle$ values for the Xe (Ba) isotopes, respectively.

Since $\langle\hat{\sigma}_z^t\rangle = 1$ for any single-particle state, $\langle\hat{\sigma}_z^t\rangle$ can be understood as a reduction factor or a quenching factor from its single-particle estimate. In Fig. 8 the quenching factors $\langle\hat{\sigma}_z^t\rangle$ are shown. Although the factors for the proton are marginally small, those for the neutron are comparable to its intrinsic value d_n. The quenching factors take the values between 0.23 and 0.98 for Xe isotopes and the values between 0.11 and 0.98 for Ba isotopes.

V. SUMMARY AND DISCUSSION

The nuclear EDM of a specific nucleus consists of two terms: one which arises from asymmetric nuclear charge distribution and the other which is induced from the intrinsic nucleon EDM.

For the first contribution coming from the isoscalar interaction, we have for the EDM of ^{129}Xe nucleus,

$$|d_{\mathrm{N,ch}}(^{129}\mathrm{Xe})| = 7.04 \times 10^{-18}\bar{g}^{(0)} g\ e\,\mathrm{cm}. \tag{37}$$

Using a relation between the isoscalar coupling $\bar{g}^{(0)}$ and the CP-violating phase $\bar{\theta}$ in the QCD Lagrangian, $\bar{g}^{(0)} = 0.027\bar{\theta}$ [26], and adopting the standard value $g = 13.5$, we have

$$|d_{\mathrm{N,ch}}(^{129}\mathrm{Xe})| = 2.6 \times 10^{-18}\bar{\theta}\ e\,\mathrm{cm}. \tag{38}$$

TABLE II. Estimated upper limits for the nuclear EDMs which arise from asymmetric nuclear charge distribution for the lowest $1/2^+$ states of Xe isotopes in units of 10^{-27} e cm.

Nucleus	^{129}Xe	^{131}Xe	^{133}Xe	^{135}Xe
Isoscalar ($I = 0$)	0.77	0.029	0.94	0.61
Isovector ($I = 1$)	0.80	0.37	0.18	0.099
Isotensor ($I = 2$)	4.1	2.2	0.12	1.2
Nucleus	^{131}Ba	^{133}Ba	^{135}Ba	^{137}Ba
Isoscalar ($I = 0$)	0.049	2.9	3.9	5.3
Isovector ($I = 1$)	0.23	0.90	1.5	1.6
Isotensor ($I = 2$)	1.3	2.5	4.9	4.4

TABLE III. The neutron quenching factor $\langle\hat{\sigma}_z^n\rangle$ and the upper limit of the nuclear EDM d_{N} (in 10^{-26} e cm) for each nuclear $1/2_1^+$ state.

Nucleus	$\langle\hat{\sigma}_z^n\rangle$	$d_{\mathrm{N,int}}$ (upper limit)
^{129}Xe	+0.2306	0.67
^{131}Xe	+0.4644	1.3
^{133}Xe	+0.6546	1.9
^{135}Xe	+0.9777	2.8
^{131}Ba	+0.1090	0.32
^{133}Ba	+0.3537	1.0
^{135}Ba	+0.4360	1.3
^{137}Ba	+0.9811	2.8

Also, using the upper limit $\bar{\theta} = 3 \times 10^{-10}$ obtained by the ^{199}Hg experiment [7], we estimate the upper limit for ^{129}Xe,

$$|d_{\mathrm{N,ch}}(^{129}\mathrm{Xe})| < 7.7 \times 10^{-28}\ e\,\mathrm{cm}, \tag{39}$$

for the isoscalar contribution. Assuming that the same relation $\bar{g}^{(I)} = 0.027\bar{\theta}$ holds for the isovector and isotensor interactions, we can predict other results shown in Table II.

Now let us calculate the second contribution coming from the intrinsic nucleon EDM. In the case of ^{129}Xe, the neutron quenching factor is $\langle\hat{\sigma}_z^n\rangle = +0.2306$. Using the upper limit for the neutron EDM, $|d_n| < 2.9 \times 10^{-26}$ e cm [27], we predict the upper limit for the nuclear EDM of ^{129}Xe:

$$|d_{\mathrm{N,int}}(^{129}\mathrm{Xe})| < 6.7 \times 10^{-27}\ e\,\mathrm{cm}, \tag{40}$$

which is nearly the upper limit of the experimentally observed atomic EDM [8], $|d(^{129}\mathrm{Xe})| < 4.1 \times 10^{-27}$ e cm. The results for other nuclear EDMs are shown in Table III.

In summary the electric dipole moments (EDMs) for the lowest $1/2^+$ states of Xe isotopes are calculated in terms of the nuclear shell model, which includes two-body nucleon interactions violating parity and time-reversal invariance. In addition, using the wave functions thus obtained, the nuclear EDMs arising from the intrinsic nucleon EDMs are calculated. The upper limits for the nuclear EDM of the Xe and Ba isotopes are estimated.

ACKNOWLEDGMENTS

We would like to express our sincere gratitude to Prof. T. Fujita for discussion and comments. The numerical calculations financially supported by Saitama University were carried out partly by the Hitachi SR16000 supercomputers at the Supercomputing Division, Information Technology Center, University of Tokyo. This work was supported by a Grant-in-Aid for Scientific Research (C) (No. 24540251) and (No. 25400267) from the Japan Society for the Promotion of Science (JSPS).

[1] M. Kobayashi and T. Maskawa, Prog. Theor. Phys. **49**, 652 (1973).
[2] A. G. Cohen, D. B. Kaplan, and A. E. Nelson, Annu. Rev. Nucl. Part. Sci. **43**, 27 (1993).
[3] M. Trodden, Rev. Mod. Phys. **71**, 1463 (1999).
[4] R. Fleischer, Phys. Rep. **370**, 537 (2002).
[5] J. S. M. Ginges and V. V. Flambaum, Phys. Rep. **397**, 63 (2004).
[6] M. Pospelov and A. Ritz, Ann. Phys. (NY) **318**, 119 (2005).
[7] W. C. Griffith, M. D. Swallows, T. H. Loftus, M. V. Romalis, B. R. Heckel, and E. N. Fortson, Phys. Rev. Lett. **102**, 101601 (2009).
[8] M. A. Rosenberry and T. E. Chupp, Phys. Rev. Lett. **86**, 22 (2001).
[9] A. Yoshimi *et al*., Phys. Lett. A **376**, 1924 (2012).
[10] S. Oshima, Phys. Rev. C **81**, 038501 (2010).
[11] C. Itoi and S. Oshima, J. Phys. Soc. Jpn. **79**, 103201 (2010).
[12] L. I. Schiff, Phys. Rev. **132**, 2194 (1963).
[13] V. V. Flambaum and A. Kozlov, Phys. Rev. A **85**, 022505 (2012).
[14] T. Fujita and S. Oshima, J. Phys. G **39**, 095106 (2012).
[15] N. Yoshinaga, K. Higashiyama, R. Arai, and E. Teruya, Phys. Rev. C **87**, 044332 (2013).
[16] N. Yoshinaga, K. Higashiyama, and R. Arai, Prog. Theor. Phys. **124**, 1115 (2010).
[17] K. Higashiyama, N. Yoshinaga, and K. Tanabe, Phys. Rev. C **67**, 044305 (2003).
[18] N. Yoshinaga and K. Higashiyama, Phys. Rev. C **69**, 054309 (2004).
[19] K. Higashiyama and N. Yoshinaga, Phys. Rev. C **83**, 034321 (2011).
[20] Z. Zhao, J. Yan, A. Gelberg, R. Reinhardt, W. Lieberz, A. Dewald, R. Wirowski, K. O. Zell, and P. von Brentano, Z. Phys. A **331**, 113 (1988).
[21] Y. Tendow, Nucl. Data Sheets **77**, 631 (1996).
[22] Yu. Khazov, I. Mitropolsky, and A. Rodionov, Nucl. Data Sheets **107**, 2715 (2006).
[23] W. C. Haxton and E. M. Henley, Phys. Rev. Lett. **51**, 1937 (1983).
[24] P. Herczeg, Hyperfine Interact. **43**, 77 (1988).
[25] P. Herczeg, Hyperfine Interact. **75**, 127 (1992).
[26] R. J. Crewther, P. Di Vecchia, G. Veneziano, and E. Witten, Phys. Lett. B **88**, 123 (1979); **91**, 487 (1980).
[27] C. A. Baker *et al*., Phys. Rev. Lett. **97**, 131801 (2006).